SHAPE-MEMORY POLYMER COMPOSITES SELECTIVELY RESPONSIVE TO NEAR-INFRARED LIGHTS OF TWO WAVELENGTHS

Tianyu Fang[1,2,3], Shunping Chen[1,2,3], Liang Fang[1,2,3,*], Zhongzi Xu[1,2,3] and Chunhua Lu[1,2,3]

[1] State Key Laboratory of Materials-Oriented Chemical Engineering, College of Materials Science and Engineering, Nanjing Tech University, Nanjing 210009, P. R. China.
[2] Jiangsu Collaborative Innovation Center for Advanced Inorganic Function Composites, Nanjing Tech University, Nanjing 210009, P. R. China.
[3] Jiangsu National Synergetic Innovation Center for Advanced Materials (SICAM), Nanjing Tech University, Nanjing 210009, PR China.
[*]: Lfang@njtech.edu.cn

Keywords: Shape-memory polymer, Rare earth organic complexes, Near-infrared light, Smart materials, Functional polymer composites

ABSTRACT

Rare earth organic complexes of $Yb(TTA)_2AAPhen$ and $Nd(TTA)_2AAPhen$ were reported here as selective photothermal fillers to near infrared (NIR) lights of 980 and 808 nm, respectively. The reactive ligand of acrylic acid (AA) containing double bonds was expected to facilitate the powder dispersion in poly[ethylene-ran-(vinyl acetate)] (EVA) as a thermally-induced shape-memory polymer during the UV curing. The powders absorbed the NIR lights with certain wavelengths and converted the light energy into heat, indirectly increasing the temperature of the EVA composites. Their full shape recoveries were triggered when the temperature went beyond the switching temperature. This work introduced an approach to make use of reactive ligands to facilitate the dispersion of photothermal fillers in shape-memory polymer composites, and correspondingly provided them with the shape-memory capability upon certain NIR lights.

1 INTRODUCTION

In last decades, shape-memory polymers (SMPs) attract increasing attentions since they can be used in many fields, including biomedical devices, aerospace instruments, remote actuators, smart textiles, and so on.[1, 2] SMPs can be programmed into a pre-defined temporal shape and recall their original shape when the temperature reaches their switching temperature (T_{sw}).[3] In comparison with heat, the light as another energy source has also been used to achieve the "on-demand" stimulation of SMPs in the remote, localized, and non-contact manner.[4] So far, a direct and simple approach to create photo-responsive SMPs is to mix thermally-induced SMPs with photothermal fillers.[3, 4] The light-induced SMP composites (SMPCs) present the compelling advantages of convenient preparation and commercial feasibility over the other approach, i.e., usage of a reversible photochemical reaction. Upon the exposure toward light, the functional fillers absorb the light energy and convert it into heat, indirectly raising the temperature of the SMPCs. When the internally generated temperature goes beyond the T_{sw}, shape recovery is induced.

Metal nanostructures, especially gold nanoparticles,[5-7] have also been reported as photothermal fillers due to surface plasmon resonance. For example, a very small amount of Au nanoparticles was introduced into crosslinked polyethylene oxide which exhibited the shape deformation under the irradiation of visible light of 532 nm.[6] Besides, the visible light with the same wavelength of 532 nm, which facilitated the easy location of the beam on the samples, was also used to trigger the localized shape recovery of SMPC micropillars in a hexagonal array based on epoxy/Au nanorods.[8] As far as the UV light is concerned, a metallosupramolecular unit formed via coordinating Mebip ligands to $Zn(NTf2)_2$ was reported as the photothermal moiety to concert UV light into heat in an epoxy based SMP.[9] The *p*-aminodiphenylimide was also used to act as photothermal filler for UV light in the epoxy SMPCs as well.[10] In comparison with UV and visible light, near-infrared (NIR) light is much safer for human tissues and naked eye and thus considered as a reliable energy source to achieve the

remotely controlled shape recovery of SMPCs. The most widely reported photothermal fillers for NIR light are the carbon nanomaterials, including carbon black,[11] carbon nanotubes,[12] graphenes.[13]

The light-induced SMPs selectively responsive to a certain wavelength can be used as building blocks to realize the multi-shape variation upon sequenced light irradiations. For example, the sequential deployment of conjoint SMPCs with temporal zigzag shapes was reported.[14, 15] Also, selectively responsive fillers were also used as actuating hinge to stimulate the sequential folding of different areas of a pre-stretched SMP film via varying the irradiation order.[16, 17] So far, the combination of lights with certain wavelengths which was used to achieve multiple shape variation of not only SMPs but all light-induced smart polymers includes UV-Vis,[18] UV-NIR,[19] Vis-Vis,[17] Vis-NIR,[20] and radiofrequency (RF)-RF.[14] For example, gold colloid and nanoshells were prepared and used in the independent optical control of microfluidic valves via separate irradiation of 532 and 832 nm beams.[20] Recently, based on rare earth (RE) organic complexes, we reported a novel photothermal filler system which exhibited selective photothermal effects towards NIR lights of 980 and 808 nm.[15] More specifically, $Yb(TTA)_3Phen$ and $Nd(TTA)_3Phen$ powders were prepared and used in creating SMPCs with shape-memory effects upon a NIR-NIR irradiations of 980 and 808 nm, respectively.

In the present work, we introduced another ligand of acrylic acid (AA) into the Yb^{3+} and Nd^{3+} organic complex for the purpose of improving the dispersion of functional fillers in the thermally-induced SMP of crosslinked poly[ethylene-*ran*-(vinyl acetate)] (EVA). The filler dispersion was observed via optical images. The photothermal effects of the fillers and the composites with different filler loadings were also examined. Finally, the shape-memory behaviors of the SMPCs with selective responsiveness towards NIR lights of 980 and 808 nm were evaluated.

2 EXPRIMENTAL

2.1 MATERIALS

The α-thenoyltrifluroacetone (TTA) and 1,10-phenanthroline (Phen) were purchased from Sinopharm Chemical Reagent Company (China). The $YbCl_3 \cdot 6H_2O$ and $NdCl_3 \cdot 6H_2O$ were provided by Funing Rare Earth Industrial Company (China). Acrylic acid (AA) and Triallyl isocyanurate (TAI, 98%) were obtained from Aladdin, China. EVA (H2031, VA content = 19%) was obtained from Sumitomo Chemical Company (Japan). Benzophenone (BP, 98%) was purchased from Sigma Aldrich. All chemicals were used without further purification.

2.2 SYNTHESIS OF YB/ND$(TTA)_2$AAPHEN COMPLEXES

$YbCl_3 \cdot 6H_2O$ (10 mmol) or $NdCl_3 \cdot 6H_2O$ (10 mmol), TTA (20 mmol), AA (10 mmol) and Phen (10 mmol) were respectively dissolved in 30 mL ethanol. The ethanol solution of YbCl3·6H2O or NdCl3·6H2O was first poured into a three-necked flask at 60 ºC in a magnetic stirring water bath, before the ethanol solutions of ligands were added dropwise. The pH value of the solution was adjusted to 6-7 using 1 mol·L-1 sodium hydroxide ethanol solution, while the mixture solution was allowed to react for 6 h. Subsequently, the precipitation was obtained using centrifugation of 10000 rpm, before washing with water and ethanol for three times each and drying in a vacuum oven at 60 oC for 12 h.

2.3 MIXING AND UV CURING

The mixing and UV curing procedures has been described schematically in a previous report. Solution casting methods were used to fabricate composite films. $Yb(TTA)_2AAPhen$ or $Nd(TTA)_2AAPhen$ was introduced into THF respectively and sonicated for 30 min. The EVA pellets, TAI (4 phr) and BP (4 phr) were added into the solution subsequently. The whole solution was stirred vigorously at 60 °C for 1 h. Next, the solution was poured into a Teflon mold, allowing the solvent evaporation naturally for at least 72 h. The obtained film was then placed into a vacuum oven at room temperature for another 24 h. Different powder loadings (2.5, 5, and 10 phr) were used in this case. The obtained film was placed between two glass plates, while the top plate was treated by mold-release agent (Trichloro(1H, 1H, 2H, 2H-perfluorooctyl)silane, J&K Chemical, China) and a Teflon film was placed between the material and the bottom plate to avoid sticking. The whole system was

pressed by office clamps and heated at 140 °C for 10 min to achieve a thin film (thickness ~ 0.6 mm). UV light of 125 W was irradiated through the transparent top plate for 1 h to allow curing.

2.4 CHARACTERIZATIONS

Microscopy. An optical microscope (BA210, Motic China Group Co., Ltd.) was used to characterize the powder dispersion in EVA matrix. The morphologies of $Yb(TTA)_2AAPhen$ and $Nd(TTA)_2AAPhen$ powders were examined using a scanning electron microscopy (SEM, JSM-6510, JOEL, Japan).

Photothermal Effect. The NIR lights of 980 and 808 nm were generated by a laser diode driver (KS3-11312-912, BWT Co., China) and a laser driver (FC-808-10W, Xinchanye Co., China), respectively. The sample temperatures were measured using a hand-held infrared camera (Xintest Company, China). The power density was determined using an optical power/energy meter (Model 1918-R, Newport, USA) equipped with a thermopile detector (Model 818P-020-12, Newport, USA).

Shape-Memory Effect. The shape-memory effect was determined on the basis of angle variation. The test specimen was placed onto a hot plate at 120 °C. After 5 min, the specimens were completely folded to 90° against a perpendicular glass plate tightly and kept for another 5 min before natural cooling to room temperature. Under the irradiation of NIR light, the instantaneous angles, θ, between the real-time location and the primary location of the bended leg were characterized with the error of ±2°. The shape recovery ratio, R_r, is determined as $R_r = \theta/90° \times 100\%$.

3 RESULTS AND DISCUSSION

Figure 1a and 1b present the chemical structures of the prepared $Yb(TTA)_2AAPhen$ or $Nd(TTA)_2AAPhen$ powders. The existence of AA as the reactive ligand is expected to facilitate the dispersion of powders in polymer matrix. The pristine $Yb(TTA)_2AAPhen$ and $Nd(TTA)_2AAPhen$ presented powder-shaped and sheet-shaped structures with the size up to ~20 μm, as shown in Figure 1c and 1d. After the UV curing reaction, the uniform dispersion of the organic complexes in EVA was observed. As shown in Figure 1e and 1f, no evident agglomerations were observed.

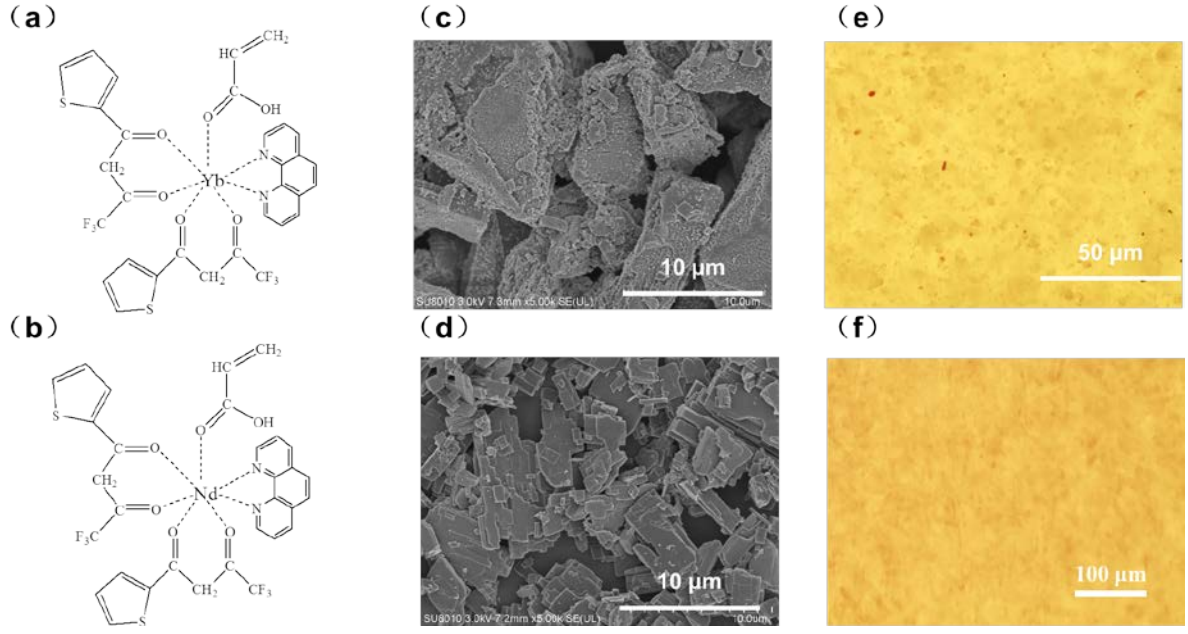

Figure 1. (a,b) Chemical structures of (a) $Yb(TTA)_2AAPhen$ and (d) $Nd(TTA)_2AAPhen$. (c,d) SEM images of (a) $Yb(TTA)_2AAPhen$ and (d) $Nd(TTA)_2AAPhen$ powders. (e,f) OM images EVA composites containing 10 phr (e) $Yb(TTA)_2AAPhen$ and (f) $Nd(TTA)_2AAPhen$

The photothermal effect of the powders was investigated subsequently. As shown in Figure 2, $Yb(TTA)_2AAPhen$ and $Nd(TTA)_2AAPhen$ powders possessed the selective photothermal effect upon the NIR lights of 980 and 808 nm, respectively. Determined by both light wavelengths and power

densities (0.2, 0.3 and 0.4 W·cm^{-2}), the temperatures of the two powders varied greatly. Upon NIR light of 980 nm with a power density of 0.2 W·cm^{-2}, the temperature of Yb(TTA)$_2$AAPhen increased evidently from room temperature to 66 °C in 60 s (Figure 1a).. The balanced temperatures were further increased to 76 and 102 °C when the powder density was 0.3 and 0.4 W·cm^{-2}. The temperature of Nd(TTA)$_2$AAPhen, however, did not change evidently. In addition, Yb(TTA)$_2$AAPhen showed no photothermal effect either upon NIR light of 808 nm. An obvious temperature increase to 55, 89, and 128 °C was observed for Nd(TTA)$_2$AAPhen upon the irradiation with the power densities of 0.2, 0.3 and 0.4 W·cm^{-2} in 60 s (Figure 2b).

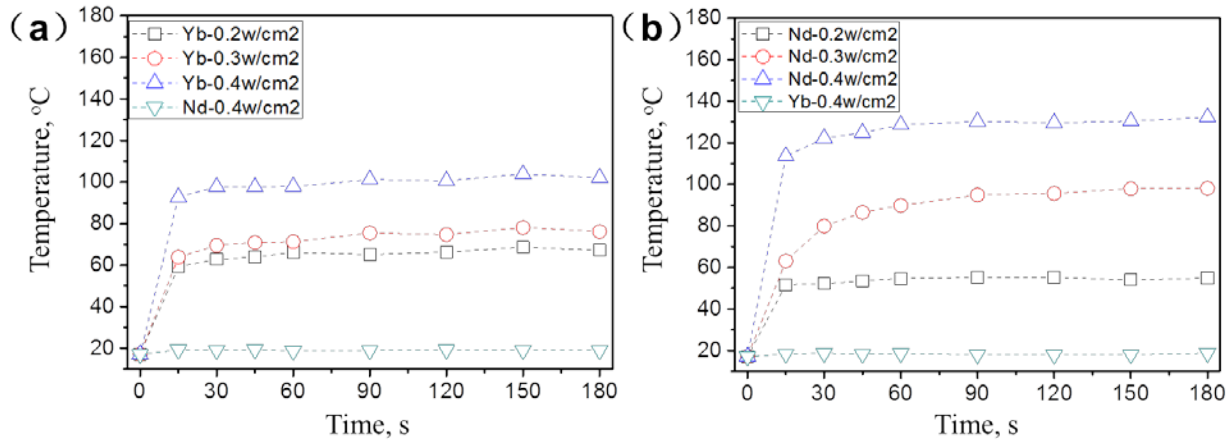

Figure 2. The temperature increase of the powders with time upon the irradiation of (a) 980 and (b) 808 nm NIR light.

The balanced temperature of the EVA/Yb(TTA)$_2$AAPhen composites in 3 min increased greatly with light PD and powder content upon the irradiation of NIR light of 980 nm (Fig. 3a). For the loading of 2.5, 5, and 10 phr, the temperature increased linearly from room temperature to 53, 60, and 102 °C at the PD of 2 W·cm^{-2}. The 10 phr Nd(TTA)$_2$AAPhen, however, increased the temperature slightly to only 47 °C at the same PD. Similarly, as shown in Fig. 3b, the composite temperature increased with light PD in a linear manner and with powder content. The loading of 2.5, 5, and 10 phr powders resulted in the temperature rise to 51, 58, and 96 °C at the PD of 0.8 W·cm^{-2}. The 10 phr Yb(TTA)$_2$AAPhen showed neglected effect on temperature increase, i.e., the balanced temperature was only 37 °C. These results clearly suggested that the introduction of Yb(TTA)$_2$AAPhen and Nd(TTA)$_2$AAPhen offered the composites selective photothermal capability for 980 and 808 nm, bringing in the selectively responsive shape-memory effect which is examined next.

At T_{deform} = 120 °C the EVA composite films with different contents of Yb(TTA)$_2$AAPhen and Nd(TTA)$_2$AAPhen powders were bended to 90° and cooled down to room temperature to fix the temporary shape. NIR light of 980 and 808 nm were irradiated onto those samples, while the shape recovery rate (*R*r) was calculated and shown in Fig. 3c and 3d. Because Nd(TTA)$_2$AAPhen did not own the photothermal capability for 980 nm, the shape recovery was not observed in EVA composite with 10 phr Nd(TTA)$_2$AAPhen. The EVA/Yb(TTA)$_2$AAPhen composites, on the other hand, performed the shape recovery under irradiation of 980 nm, particularly at the loading of 5 and 10 phr. Since the temperature increase was enhanced at a higher content, EVA composites with 10 phr Yb(TTA)$_2$AAPhen reached full recovery at a smaller PD than the one with 5 phr Yb(TTA)$_2$AAPhen. The NIR light of 808 nm instead did not trigger the shape change of Yb(TTA)$_2$AAPhen with 10 phr loading (Fig. 3d). Only the powder of Nd(TTA)$_2$AAPhen can realize the shape recovery under the irradiation of 808 nm NIR light, while higher content (10 phr) also trigger the recovery under a smaller PD. Because of the selective photothermal effect of Yb(TTA)$_2$AAPhen and Nd(TTA)$_2$AAPhen powders, their composites with EVA presented the shape recovery to the certain wavelength of 980 and 808 nm, respectively.

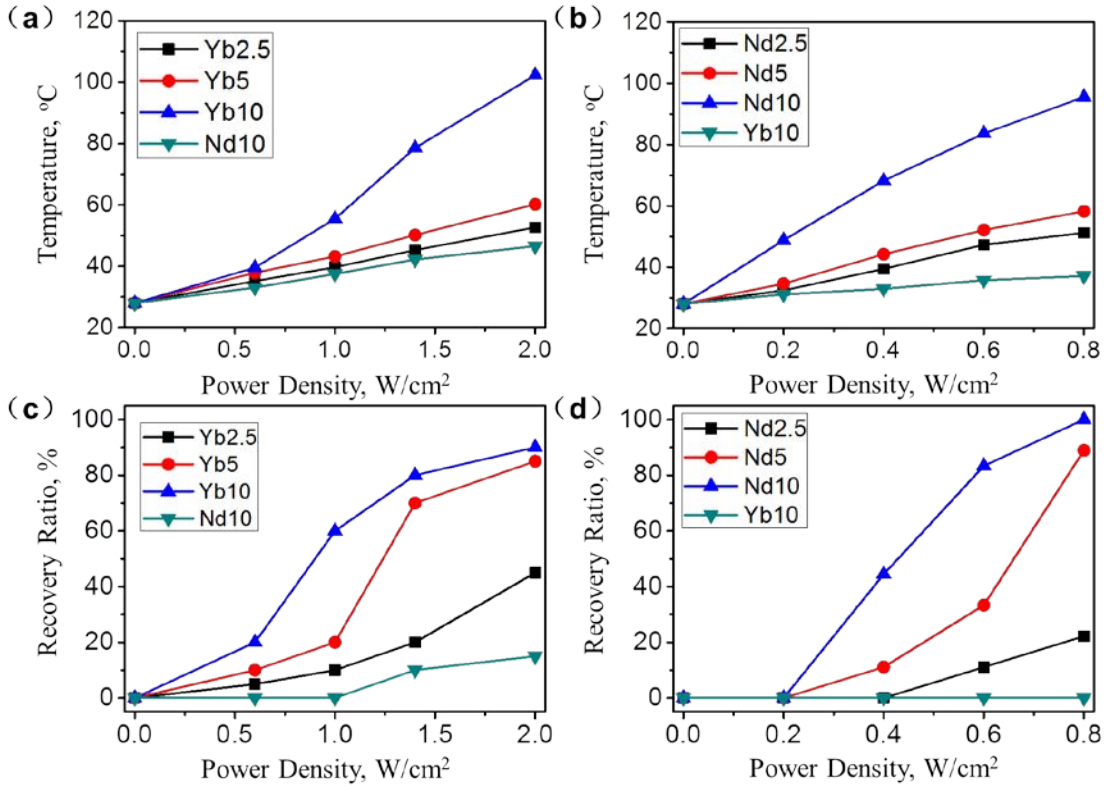

Figure 3. (a-b) Photothermal effect and (c-d) shape recovery ratio of EVA composites with different loading of $Yb(TTA)_2AAPhen$ and $Nd(TTA)_2AAPhen$ under the irradiation of NIR light with (a, c) 980 and (b, d) 808 nm.

4 CONCLUSIONS

Acrylic acid (AA) was introduced as reactive ligand into rare earth organic complexes of $Yb(TTA)_2AAPhen$ and $Nd(TTA)_2AAPhen$ to facilitate their dispersion in poly[ethylene-ran-(vinyl acetate)] (EVA) as a thermally-induced shape-memory polymer during in-situ UV curing. The two powders presented selective photothermal effect for near infrared lights of 980 and 808 nm and accordingly provided the prepared composites with selective responsivity. Good shape recoveries were realized when the increased temperature reached the switching temperature of the composites.

ACKNOWLEDGEMENTS

This work was sponsored by the Scientific Research Foundation for Returned Scholars (ZX15504320001), National Natural Science Foundation of China (51503098), and Preferred Program Foundation for Returned Scholars (ZX15512320008). The Priority Academic Program Development of the Jiangsu Higher Education Institutions (PAPD) is appreciated.

REFERENCES

[1]. Q. Zhao, H.J. Qi, T. Xie, Recent progress in shape memory polymer: New behavior, enabling materials, and mechanistic understanding, *Progress in Polymer Science*, **49**, 2015, pp. 79-120.
[2]. J. Hu, Y. Zhu, H. Huang, J. Lu, Recent advances in shape–memory polymers: Structure, mechanism, functionality, modeling and applications, *Progress in Polymer Science*, **37**, 2012, pp. 1720-1763.
[3]. J. Leng, X. Lan, Y. Liu, S. Du, Shape-memory polymers and their composites: Stimulus methods and applications, *Progress in Materials Science*, **56**, 2011, pp. 1077-1135.
[4]. D. Habault, H. Zhang, Y. Zhao, Light-triggered self-healing and shape-memory polymers, *Chemical Society Reviews*, **42**, 2013, pp. 7244.

[5]. H. Zhang, H. Xia, Y. Zhao, Optically triggered and spatially controllable shape-memory polymer–gold nanoparticle composite materials, *J. Mater. Chem.*, **22**, 2012, pp. 845-849.
[6]. H. Zhang, Y. Zhao, Polymers with Dual Light-Triggered Functions of Shape Memory and Healing Using Gold Nanoparticles, *ACS Applied Materials & Interfaces*, **5**, 2013, pp. 13069-13075.
[7]. H. Zhang, H. Xia, Y. Zhao, Light-Controlled Complex Deformation and Motion of Shape-Memory Polymers Using a Temperature Gradient, *ACS Macro Letters*, **3**, 2014, pp. 940-943.
[8]. Y. Zheng, J. Li, E. Lee, S. Yang, Light-induced shape recovery of deformed shape memory polymer micropillar arrays with gold nanorods, RSC Adv., 5 (2015) 30495-30499.
[9]. Y. Wu, J. Hu, C. Zhang, J. Han, Y. Wang, B. Kumar, A facile approach to fabricate a UV/heat dual-responsive triple shape memory polymer, *J. Mater. Chem. A*, **3**, 2015, pp. 97-100.
[10]. Y. Chen, H. Yu, M. Quan, L. Zhang, H. Yang, Y. Lu, Photothermal effect of azopyridine compounds and their applications, *RSC Adv.*, **5**, 2015, pp. 4675-4680.
[11]. J. Leng, X. Wu, Y. Liu, Infrared light-active shape memory polymer filled with nanocarbon particles, *Journal of Applied Polymer Science*, **114**, 2009, pp. 2455-2460.
[12]. H. Lu, Y. Yao, W.M. Huang, J. Leng, D. Hui, Significantly improving infrared light-induced shape recovery behavior of shape memory polymeric nanocomposite via a synergistic effect of carbon nanotube and boron nitride, *Composites Part B: Engineering*, **62**, 2014, pp. 256-261.
[13]. L. Zhou, Q. Liu, X. Lv, L. Gao, S. Fang, H. Yu, Photoinduced triple shape memory polyurethane enabled by doping with azobenzene and GO, *J. Mater. Chem. C*, **4**, 2016, 9993-9997.
[14]. Z. He, N. Satarkar, T. Xie, Y.T. Cheng, J.Z. Hilt, Remote controlled multishape polymer nanocomposites with selective radiofrequency actuations, *Advanced Materials*, **23**, 2011, pp. 3192-3196.
[15]. L. Fang, S. Chen, T. Fang, J. Fang, C. Lu, Z. Xu, Shape-memory polymer composites selectively triggered by near-infrared light of two certain wavelengths and their applications at macro-/microscale, *Composites Science and Technology*, **138**, 2017, pp. 106-116.
[16]. Y. Liu, J.K. Boyles, J. Genzer, M.D. Dickey, Self-folding of polymer sheets using local light absorption, *Soft Matter*, **8**, 2012, pp. 1764-1769.
[17]. Y. Liu, B. Shaw, M.D. Dickey, J. Genzer, Sequential self-folding of polymer sheets, *Science Advances*, **3**, 2017, pp. e1602417.
[18]. M. Wang, B.P. Lin, H. Yang, A plant tendril mimic soft actuator with phototunable bending and chiral twisting motion modes, *Nature Communications*, **7**, 2016, pp. 13981.
[19]. Z. Cheng, T. Wang, X. Li, Y. Zhang, H. Yu, NIR-Vis-UV Light-Responsive Actuator Films of Polymer-Dispersed Liquid Crystal/Graphene Oxide Nanocomposites, *ACS Applied Materials & Interfaces*, **7**, 2015, pp. 27494-27501.
[20]. S.R. Sershen, G.A. Mensing, M. Ng, N.J. Halas, D.J. Beebe, J.L. West, Independent optical control of microfluidic valves formed from optomechanically responsive nanocomposite hydrogels, *Advanced Materials*, **17**, 2005, pp. 1366-1368.